LAWRENCE
LIVERMORE
NATIONAL
LABORATORY

UCRL-JRNL-219888

Comparisons Between Experimental Measurments and Numerical Simulations of Spheromak Formation in SSPX

C. A. Romero-Talamás, E. B. Hooper, D. N. Hill, B. I. Cohen, H. S. McLean, R. D. Wood, J. M. Moller

March 17, 2006

Journal of Fusion Energy

Comparisons Between Experimental Measurements and Numerical Simulations of Spheromak Formation in SSPX

C. A. Romero-Talamás* and E. B. Hooper, D. N. Hill,

B. I. Cohen, H. S. McLean, R. D. Wood, J. M. Moller

Lawrence Livermore National Laboratory,

7000 East Avenue, Livermore, California, 94550.†

(Dated: March 15, 2006)

Abstract

Data from a recently installed insertable magnetic probe array in the Sustained Spheromak Physics Experiment (SSPX) [E. B. Hooper et al., Nucl. Fusion **39**, 863 (1999)] is compared against NIMROD [C. R. Sovinec et al., J. Comp. Phys. **195**, 355 (2004)], a full 3D resistive magnetohydrodynamic code that is used to simulate SSPX plasmas. The experiment probe consists of a linear array of chip inductors arranged in clusters that are spaced every 2 cm, and spans the entire machine radius at the flux conserver midplane. Both the experiment and the numerical simulations show the appearance, shortly after breakdown, of a column with a hollow current profile that precedes magnetic reconnection, a process essential to the formation of closed magnetic flux surfaces. However, there are differences between the experiment and the simulation in how the column evolves after it is formed. These differences are studied to help identify the mechanisms that eventually lead to closed-flux surfaces (azimuthally averaged) and flux amplification, which occur in both the experiment and the simulation.

*Electronic address: romerotalamas1@llnl.gov

†This work performed under the auspices of the USDOE by LLNL under contract 7405-Eng-48.

I. INTRODUCTION

The Sustained Spheromak Physics Experiment (SSPX) [1] is aimed at understanding how currents in the plasma produce the spheromak, and the efficiency with which spheromak fields contain hot plasmas. Diagnostics for this machine include, among others: CO2 interferometers, Thomson scattering, edge magnetics [2–4], high-speed imaging [5, 6], and more recently, an insertable magnetic probe of similar construction as the one reported in Ref. [7]. Data from this probe is used to compare against NIMROD [8], a full three-dimensional magnetohydrodynamic code that is used to simulate SSPX plasmas.

The motivation to study the evolution of SSPX plasma shortly after breakdown is to understand the transition from open to closed magnetic flux surfaces. That is, when topology changes through magnetic reconnection and forms a spheromak. Exactly where and when magnetic reconnection occurs to produce this transition is still unknown. At present, there are two hypotheses. One is based on NIMROD simulations and predicts the development of chaotic field structures in which reconnection can occur in multiple locations in the plasma volume before relaxing to the approximately force-free state (i.e., $\mathbf{J} \parallel \mathbf{B}$). The other hypothesis is based on the initial transient column kinking and developing two full turns or more before reconnecting at a single location (see [5] and references therein). High-speed images have shown the transient column kinking in time-scales of microseconds. However, the ionization percentage increases rapidly precisely at the onset of kinking and the amount of visible light that the camera captures decreases accordingly, resulting in images too low in contrast (or blurred if the shutter is left open for too long) to be able to count the turns in the kink.

II. EARLY MAGNETIC EVOLUTION IN SSPX AND NIMROD

To study the early formation of SSPX plasmas, a probe containing miniature chip inductors was inserted into the flux conserver. Figure 2 shows the location of the probe in the flux conserver. In the lower left of the figure, a photograph is shown of a cluster of chip inductors that measure B_r, B_θ, and B_z. The inductors are placed inside a vacuum-tight enclosure covered in boron nitride. Twenty-one clusters spaced every 2 cm were used in the measurements presented here. The vector plots represent the toroidal and poloidal projections of

the magnetic field (not scaled in magnitude, only in orientation), taken every microsecond. The high-speed images shown on the right of the figure were taken simultaneously to the magnetic measurements.

Comparing with the plasma images in Figure 1, the vector plots show that as the plasma expands into the flux conserver, the gun current (already hundreds of kiloamperes) is carried along a thin sheet that evolves into a central column with a hollow current profile. That is, B_θ is zero inside the column, consistent with zero current along the column. Conversely, outside the column only B_θ is non-zero, consistent with no toroidal currents in this region.

The current sheet behavior is also seen in NIMROD. Figure 3 shows a comparison of the same magnetic signals shown in Figure 2 (the signals are interpolated and scaled in magnitude). The time at which the expanding plasma first touches the probe (reaches midplane) is $t_{rel} = 0$. Before that, the magnitude of the signals is extremely small in both the experiment and the simulation. Although the simulation is qualitatively the same as SSPX in the first few microseconds, the SSPX plasma expands faster into the flux conserver. This is indicated by the letter **A** in Figure 3. At $t_{rel} = 7.53\mu s$ the central column keeps decreasing in diameter, and continues to be smaller than in the simulation.

The most important difference between experiment and simulation occurs at $t_{rel} = 13.2\mu s$. At this time, B_z signals (approximately equal to B poloidal) start to appear inside the bubble that is formed by the current sheet (indicated by the letter **B**), whereas in the experiment these signals are essentially zero. This is indicative of toroidal currents appearing inside the expanding bubble sooner in NIMROD than in SSPX. In the SSPX signals, however, the relative amplitude of the $|B|$ field oscillations is greater than in NIMROD, indicating a strong kink in the central column.

At $t_{rel} = 22.6\mu s$ the signals are again qualitatively the same. The sign reversal in B_z indicates that a toroidal current flows along the magnetic axis which is located either above or below the radial location at which $B_z = 0$ (approximately $R = 0.33m$).

III. DISCUSSION

The comparison presented here shows the similarities and differences in SSPX and NIMROD during the early spheromak formation process. In SSPX the relative amplitude of magnetic oscillations is higher than in NIMROD, indicating that the central column kinks

significantly more than in NIMROD. The diameter of this column also seems to be smaller in SSPX. The data, however, is not sufficient to discern the mechanisms that lead to the formation of closed flux surfaces. It is possible, however, that both hypotheses mentioned in Section I lead to the formation of a spheromak.

It should be noted here that NIMROD is a single-fluid magnetohydrodynamic code that does not contain any of the atomic physics such as line radiation and plasma-wall interactions, which are ever present in the experiment, especially during the formation phase. Due to limitations in the numerics, the code also assumes that plasma pre-fills the machine volume and cannot have a plasma-vacuum boundary. This condition is likely to be responsible for the appearance of current inside the expanding bubble (Figure 4), and thus creates poloidal magnetic signals that appear sooner than in the experiment. These internal currents, in turn, are alternative paths for the gun current and reduce the current flowing through the central column, reducing the possibility of driving the column kink-unstable.

---

[1] E. B. Hooper, L. D. Pearlstein, and R. H. Bulmer. *Nucl. Fusion*, 39:863, 1999.

[2] H. S. McLean, A. Ahmed, D. Buchenauer, et al. *Rev. Sci. Instrum.*, 72:556, 2001.

[3] Z. Wang, G. A. Wurden, C. W. Barnes, C. J. Buchenauer, H. S. McLean, D. N. Hill, E. B. Hooper, R. D. Wood, and S. Woodruff. *Rev. Sci. Instrum.*, 72(1):1059, 2001.

[4] Y. Roh, C. W. Domier, and N. C. Luhmann Jr. *Rev. Sci. Instrum.*, 74(3):1518, 2003.

[5] C. A. Romero-Talamás, C. Holcomb, P. M. Bellan, and D. N. Hill. *Phys. Plasmas*, 13:022502, 2006.

[6] C. A. Romero-Talamás. *Investigations of spheromak plasma dynamics: high-speed imaging at the sustained spheromak physics experiment and magnetic diagnostics at the Caltech spheromak experiment.* PhD thesis, California Institute of Technology, Pasadena, California, 2005.

[7] C. A. Romero-Talamás, P. M. Bellan, and S. C. Hsu. *Rev. Sci. Instrum.*, 75:2664, 2004.

[8] C. R. Sovinec, A. H. Glasser, T. A. Gianakon, D. C. Barnes, R. A. Nebel, S. E. Kruger, D. D. Schnack, S. J. Plimpton, A. Tarditi, and M. S. Chu. *J. Comp. Phys.*, 195:355, 2004.

This work was performed under the auspices of the U.S. Department of Energy by University of California, Lawrence Livermore National Laboratory under Contract W-7405-Eng-48.

IV. FIGURE CAPTIONS

- Figure 1. Plasma breakdown and ballooning sequence. Immediately after breakdown, plasma travels down the gun and into the flux conserver. The camera captures the expanding plasma as soon as it enters the flux conserver. The rightmost image shows a faint column kinking, which typically occurs in less than 10 μs after the central column is formed. Diagnostics, including the high-speed camera, access the plasma through the opening shown on the image of the flux conserver with no plasma (upper right). The horizontal field of view is almost 1 m, and images are taken in the visible range (light is mostly H_α).

- Figure 2. The frames on the left show the probe location in the flux conserver and the chip inductors used inside the probe. The vector plots shown here are the toroidal and poloidal projections of the vector field along the array, plotted every $1\mu s$ after the plasma first touches the probe . Each vector in the plots correspond to one of the 21 clusters used in these measurements.

- Figure 3. Comparison between magnetic signals in SSPX (shot 15261) and NIMROD (lam07). The relative time $t_{rel} = 0$ is the time at which the expanding plasma first touches the probe (or arrives at midplane in the case of NIMROD). The vertical axes are in units of Tesla, and the horizontal axes in meters.

- Figure 4. Current density plot in NIMROD showing the formation of filaments inside the expanding bubble. The current flowing along the sheet is of the order of a few MA/m^2. The frame on the right corresponds to t_{rel} $0\mu s$.

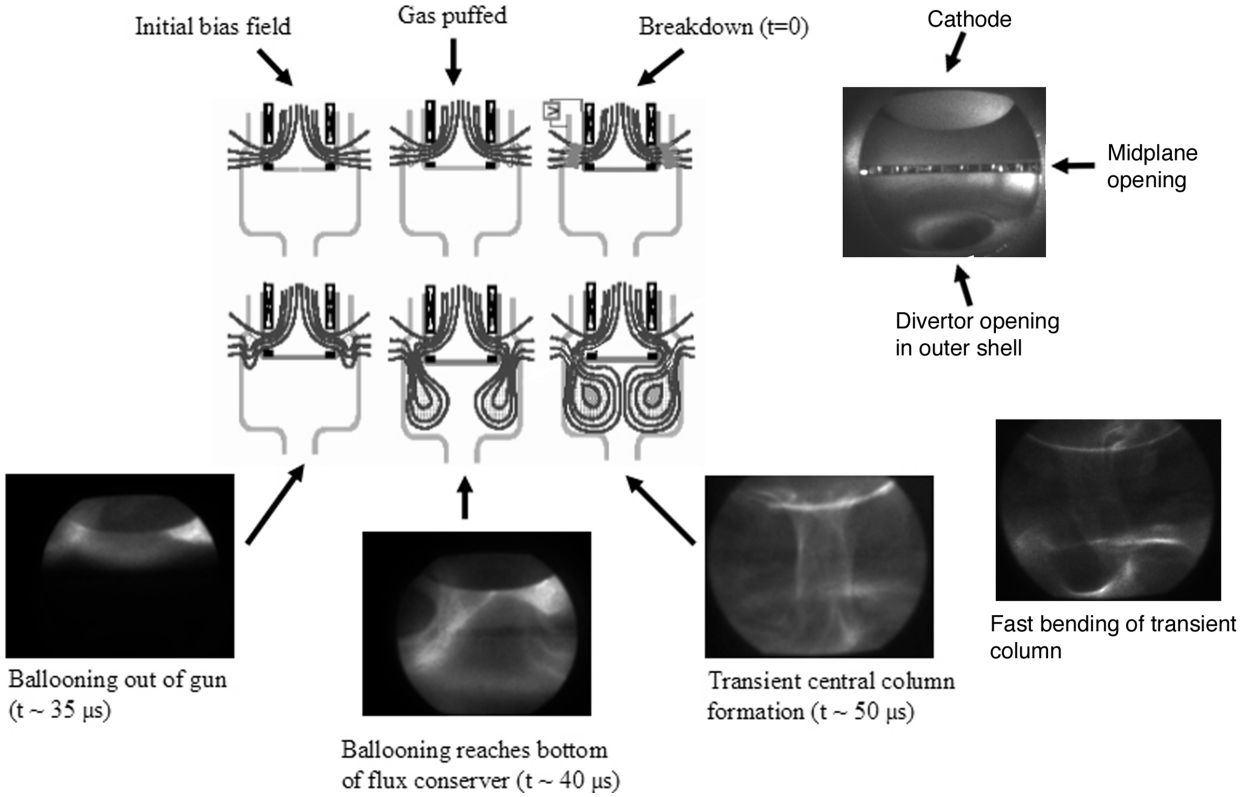
Initial bias field
Gas puffed
Breakdown (t=0)
Cathode
Midplane opening
Divertor opening in outer shell
Ballooning out of gun (t ~ 35 μs)
Ballooning reaches bottom of flux conserver (t ~ 40 μs)
Transient central column formation (t ~ 50 μs)
Fast bending of transient column

FIG. 1:

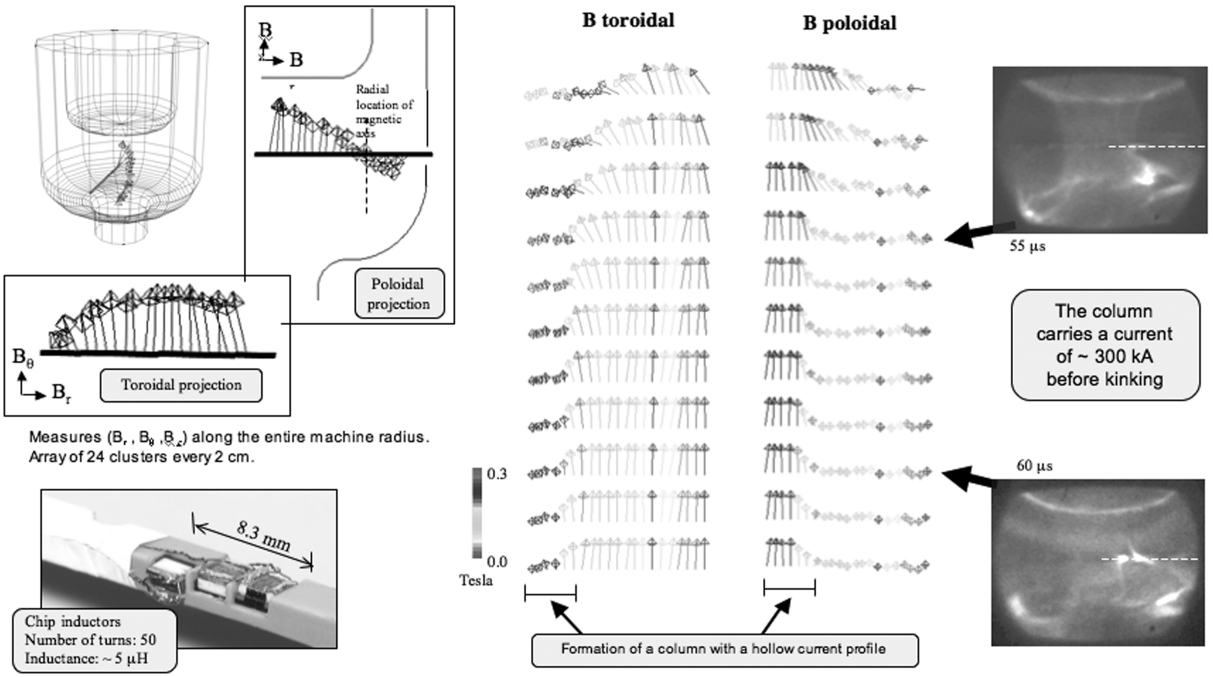
B toroidal
B poloidal
Radial location of magnetic axis
Poloidal projection
Toroidal projection
Measures (B, , B , B) along the entire machine radius.
Array of 24 clusters every 2 cm.
8.3 mm
Chip inductors
Number of turns: 50
Inductance: ~ 5 μH
0.3
0.0
Tesla
55 μs
60 μs
The column carries a current of ~ 300 kA before kinking
Formation of a column with a hollow current profile

FIG. 2:

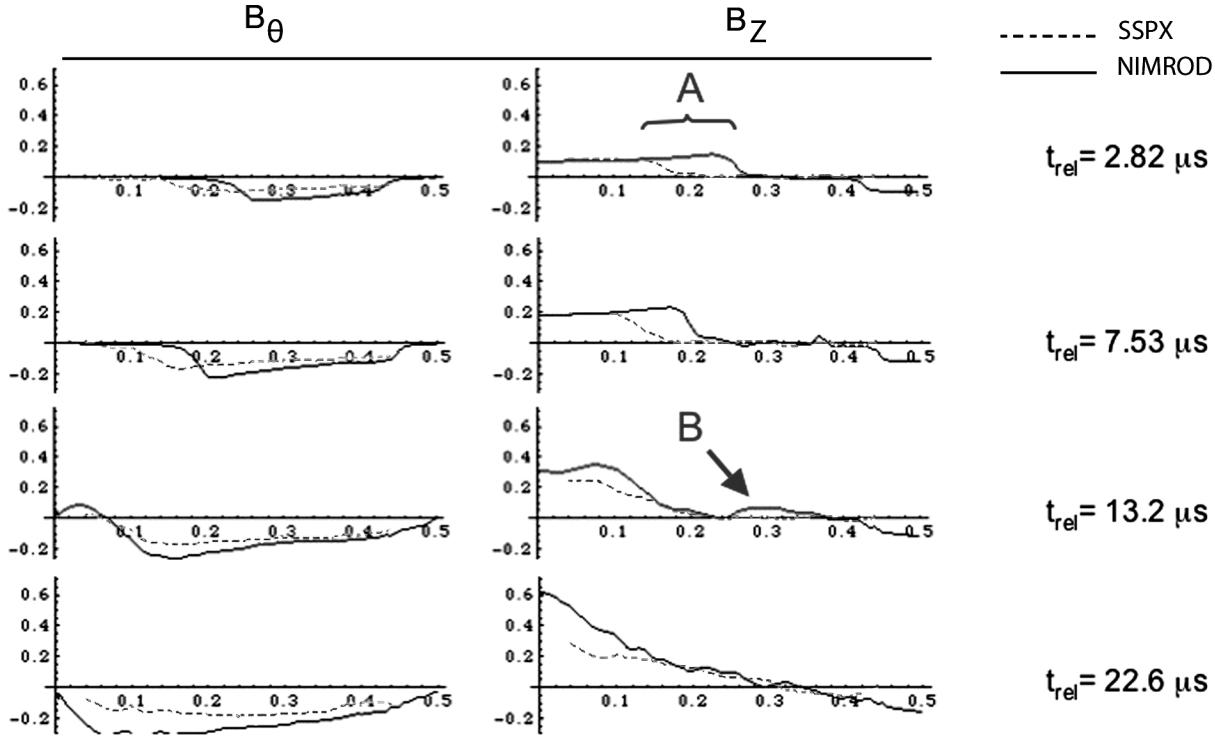
B_θ
B_Z
SSPX
NIMROD
A
B
t_{rel}= 2.82 μs
t_{rel}= 7.53 μs
t_{rel}= 13.2 μs
t_{rel}= 22.6 μs

FIG. 3:

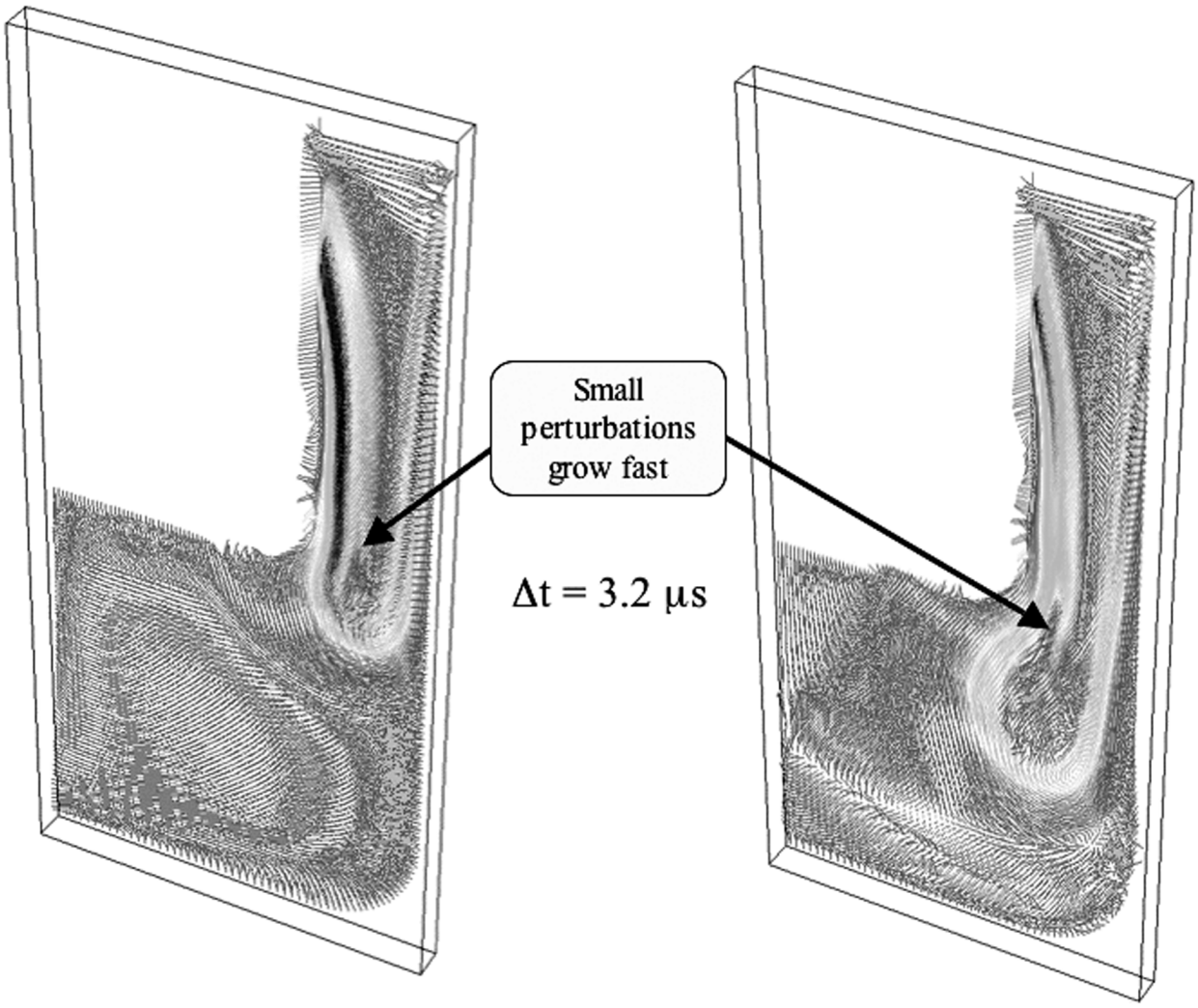

FIG. 4: